Author/s:
Grogan, LF;Cashins, SD;Skerratt, LF;Berger, L;McFadden, MS;Harlow, P;Hunter, DA;Scheele, BC;Mulvenna, J

Title:
Evolution of resistance to chytridiomycosis is associated with a robust early immune response

Date:
2018-02-01

Citation:
Grogan, L. F., Cashins, S. D., Skerratt, L. F., Berger, L., McFadden, M. S., Harlow, P., Hunter, D. A., Scheele, B. C. & Mulvenna, J. (2018). Evolution of resistance to chytridiomycosis is associated with a robust early immune response. Molecular Ecology, 27 (4), pp.919-934. https://doi.org/10.1111/mec.14493.

DR. LAURA FRANCES GROGAN (Orcid ID : 0000-0002-2553-7598)

Article type : Original Article

Evolution of resistance to chytridiomycosis is associated with a robust early immune response

Laura F. Grogan[1,2,7*], Scott D. Cashins[1], Lee F. Skerratt[1], Lee Berger[1], Michael S. McFadden[3], Peter Harlow[3], David A. Hunter[4], Ben C. Scheele[1,5] & Jason Mulvenna[6,7]

[1] One Health Research Group, College of Public Health, Medical and Veterinary Sciences, James Cook University, Angus Smith Drive, Townsville, Queensland 4811, Australia.

[2] Griffith Wildlife Disease Ecology Group, Environmental Futures Research Institute, School of Environment, Griffith University, Nathan, Queensland 4111, Australia.

[3] Taronga Conservation Society Australia, Bradleys Head Road, Mosman, NSW 2088, Australia.

[4] Ecosystems and Threatened Species, South West Region, Office of Environment and Heritage, NSW Department of Premier and Cabinet, 11 Farrer Street, Queanbeyan, NSW 2620, Australia.

[5] Fenner School of Environment and Society, Australian National University, Canberra, ACT 0200, Australia.

[6] School of Biomedical Sciences, The University of Queensland, Brisbane, QLD 4072, Australia.

[7] Genetics and Computational Biology, QIMR Berghofer Medical Research Institute, 300 Herston Road, Brisbane, Queensland 4006, Australia.

Keywords: *Batrachochytrium dendrobatidis*, chytridiomycosis, next generation sequencing, resistance, transcriptomics, gene expression

* Corresponding author
Name: Laura Grogan
Current address: Griffith Wildlife Disease Ecology Group, Environmental Futures Research Institute, School of Environment, Griffith University, Nathan, Queensland, 4111, Australia.
Tel: (+61 4) 0225 5204
Email: l.grogan@griffith.edu.au

Running title: **Chytridiomycosis and immune gene expression**

Word count: 6,753 (Introduction, Materials and Methods, Results, and Discussion)

ABSTRACT

Potentiating the evolution of immunity is a promising strategy for addressing biodiversity diseases. Assisted selection for infection resistance may enable the recovery and persistence of amphibians threatened by chytridiomycosis; a devastating fungal skin disease threatening hundreds of species globally. However, knowledge of the mechanisms involved in the natural evolution of immunity to chytridiomycosis is limited. Understanding the mechanisms of such resistance may help speed assisted-selection. Using a transcriptomics approach we examined gene expression responses of endangered alpine tree frogs (*Litoria verreauxii alpina*) to subclinical infection, comparing two long-exposed populations with a naïve population. We performed a blinded, randomized and controlled exposure experiment, collecting skin, liver and spleen tissues at 4, 8 and 14 days post-exposure from 51 wild-caught captively-reared infection-naïve adult frogs for transcriptome assembly and differential gene expression analyses. We analysed our results in conjunction with infection intensity data and the results of a large clinical survival experiment run concurrently with individuals from the same clutches. Here we show that frogs from an evolutionarily long-exposed and phenotypically more resistant population of the highly susceptible alpine tree frog demonstrate a more robust innate and adaptive immune response at the critical early subclinical stage of infection when

compared with two more susceptible populations. These results are consistent with the occurrence of evolution of resistance against chytridiomycosis, help to explain underlying resistance mechanisms, and provide genes of potential interest and sequence data for future research. We recommend further investigation of cell-mediated immunity pathways, the role of interferons and mechanisms of lymphocyte suppression.

INTRODUCTION

The emergence of biodiversity diseases that worsen the conservation status of wildlife species is of increasing global concern (Grogan *et al.* 2014). Spread of chytridiomycosis, a skin disease caused by fungal pathogen *Batrachochytrium dendrobatidis* (Bd), has devastated amphibian species around the world (Skerratt *et al.* 2007), but is now endemic in most climatically suitable regions (Fisher *et al.* 2009; Kinney *et al.* 2011; Murray *et al.* 2011). Despite endemism, many populations continue to be threatened by chytridiomycosis (Murray *et al.* 2009; Phillott *et al.* 2013; Scheele *et al.* 2015; Scheele *et al.* 2017; Skerratt *et al.* 2016). Development and implementation of *in situ* interventions for managing these populations are still in their infancy (Bosch *et al.* 2015; Scheele *et al.* 2014b). Selection for evolved resistance or tolerance to disease has been suggested as a possible strategy for promoting long-term population persistence and assisting the successful repatriation of *ex situ* captive colonies (Scheele *et al.* 2014b; Skerratt *et al.* 2016; Venesky *et al.* 2012). The evolution of resistance or tolerance has been demonstrated in other wildlife (Atkinson *et al.* 2013), such as the resistance to bacterial infection with *Mycoplasma galliseptum* in the North American house finch (*Carpodacuc mexicanus*) (Bonneaud *et al.* 2011).

Individual, population and species-level differences in susceptibility to chytridiomycosis suggest immunologic management strategies are possible (Scheele *et al.* 2014b; Searle *et al.* 2011). However, many non-immune factors also determine disease manifestation (variations in autecology, behaviour, environment and pathogen strain; Berger *et al.* 2005a; Koprivnikar *et al.* 2011; Murray & Skerratt 2012; Rowley & Alford 2007). The broad host and geographic range of chytridiomycosis has also made it difficult to draw parallels across species and systems and hence find generic solutions (Olson *et al.* 2013). The amphibian immune response to pathogens, similar to other vertebrates, is extremely complex, involving numerous

cell types and hundreds of interacting molecular pathways (Murphy 2012; Robert & Ohta 2009). This complexity makes it difficult not only to isolate the effects of individual components, but also to understand their relative importance within the whole system (Ramsey *et al.* 2010). Several immune determinants of susceptibility have been identified to date, including anti-microbial skin defense peptides, symbiotic skin bacteria and their anti-fungal metabolites, immune cells and their responses to Bd, stress metabolites, and expression of major histocompatibility complex (MHC) genes (Bataille *et al.* 2015; Berger *et al.* 2005b; Cashins *et al.* 2013; Fites *et al.* 2013; Holden & Rollins-Smith 2014; McMahon *et al.* 2014; Pask *et al.* 2013; Ramsey *et al.* 2010; Savage & Zamudio 2011; Young *et al.* 2014).

Key elements of selecting for evolved resistance to chytridiomycosis involve 1) evidence for the evolution of resistance in amphibian populations, 2) understanding the underlying mechanisms associated with evolved resistance, and 3) identification of molecular and genetic targets for marker-assisted selection (MAS) – an approach that has been successfully used for selecting disease resistance in plant and animal agriculture (Leeds *et al.* 2010; Ragimekula *et al.* 2013). Two studies have made initial progress towards these goals by examining MHC gene expression and correlating this with survival in clinical experiments and in wild populations (Bataille *et al.* 2015; Savage & Zamudio 2011), indicating likely selection for resistance at the MHC locus. While such gene-targeted approaches can yield important information about the potential evolution of resistance (Meyer & Thomson 2001), they may overlook the potentially multifactorial nature of protective immunity and other key components of the immune system that provide protection.

Dynamic gene expression in response to chytridiomycosis has been investigated with alternative non-targeted approaches in several studies (Ellison *et al.* 2014; Ellison *et al.* 2015; Price *et al.* 2015; Ribas *et al.* 2009; Rosenblum *et al.* 2012; Rosenblum *et al.* 2009), however none have examined the potential for evolution of resistance within species, nor related gene expression responses to demonstrated clinical survival. Early whole-genome microarray studies found little evidence for a robust immune response in skin, liver and spleen tissues of exposed frogs at various times since exposure (sampled at 3, 7, 16 and 42 days post exposure; DPE) in three susceptible species (*Xenopus (Silurana) tropicalis*, *Rana muscosa* and *R. sierrae*) (Ribas *et al.* 2009; Rosenblum *et al.* 2012; Rosenblum *et al.* 2009). In contrast, a

recent transcriptomics study found high expression of immune-associated transcripts in the skin and spleen of moribund (sampled at 22-33 DPE) *Atelopus zeteki* (a highly susceptible species) in conjunction with decreased expression of lymphocyte-associated transcripts in the spleen (Ellison *et al.* 2014). Furthermore, when compared with two resistant (*Craugastor fitzingeri* and *A. callidryas*) and one other susceptible species (*A. glyphus*), Ellison *et al.* (2015) found comparatively lower levels of immune response in skin and spleen tissues of resistant species at peak infection loads (sampled at 33-62 DPE), although only susceptible species demonstrated suppression of splenic T-cell genes.

These apparently conflicting levels of immune response observed between the different studies may be associated with differences in sensitivity of the methodology (the former three used microarrays; Ribas *et al.* 2009; Rosenblum *et al.* 2012; Rosenblum *et al.* 2009; while the latter two used highly sensitive RNA-seq; Ellison *et al.* 2014; Ellison *et al.* 2015), differences in the inherent susceptibility of host species investigated (Searle *et al.* 2011), or the likely presence in the latter two studies of confounding immunopathology that may occur in late-stage infection (de Graaf *et al.* 2015). Host-pathogen infection interactions are highly temporally dynamic (Huang *et al.* 2011) and are often characterized by many non-protective processes including escalating pathophysiology (disruption of homeostasis, tissue damage and bacterial co-infections) with increasing infection intensity, that may confound late stage observations (Berger *et al.* 2005b). Thus, while investigating putative immune mechanisms underlying clinically protective resistance it is important to consider early subclinical responses. A recent RNA-seq study by Price *et al.* (2015) found a stronger (albeit small) transcriptional response at 4 DPE to Bd than to *Ranavirus* in liver tissue of *Rana temporaria* (a species relatively resistant to Bd but susceptible to *Ranavirus*), however these results were not linked with clinical evidence for resistance and greater survival in individuals. These findings show that comparing the early transcriptomic response between frogs with differing clinical resistance to Bd has potential to identify novel and effective immunological changes that are not confounded by late stage immunopathology.

In this study we used a non-targeted transcriptomics approach to investigate underlying immune mechanisms that may be associated with the evolution of resistance to chytridiomycosis and may manifest in the early subclinical phase of infection. We examined

infection responses in the alpine tree frog (*Litoria verreauxii alpina*) comparing frogs from a naïve population (Grey Mare) and from two populations that had been exposed to the fungus for approximately 20 years through many generations (Kiandra and Eucumbene). Unfortunately, at the time of our study there were no other known naïve populations available, so the lack of replication of the naïve population was beyond our control. We characterized differential gene expression between wild-caught captive-raised adult frogs comparing experimentally infected and uninfected frogs between populations, sampling three different immune-associated tissues (skin, spleen and liver) at various subclinical time-points post exposure (4, 8 and 14 days). We examined infection intensities, and compared our results with survival curves from a large experiment undertaken concurrently with frogs from identical clutches (Bataille *et al.* 2015; Grogan 2014; Grogan *et al.* 2018). The novelty of our approach lies in analysing gene expression in frogs raised from naïve and long-exposed populations (approximately 8-10 generations) that were concurrently assessed for susceptibility by an infection experiment.

MATERIALS AND METHODS

Study subjects and husbandry

Fifty-one Bd-naïve adult alpine tree frogs (*L.v. alpina*) were raised in Bd-negative quarantine conditions from wild-caught egg-masses until eight months post-metamorphosis (Scientific License number: S12848). The frogs were sourced from three geographically distinct populations around Kosciuszko National Park, New South Wales, Australia (Grogan *et al.* 2018). Two of the populations (Kiandra and Eucumbene) had been long-exposed to Bd and had experienced marked declines associated with the spread of Bd in the 1980s (Osborne *et al.* 1999; Scheele *et al.* 2014a), while a third population (Grey Mare) was naïve to the pathogen (Hunter *et al.* 2009; Scheele *et al.* 2016). The tissue-response experiment described here was performed concurrent with, under identical conditions, and using frogs from the same cohort as a larger exposure study examining survival responses. That survival experiment involved an additional 355 animals from 3-4 clutches from each of four populations (99 frogs from Eucumbene, 80 frogs from Grey Mare, 100 frogs from Kiandra, and 76 frogs from an additional site Ogilvies).

Frogs were transferred to individual tubs several weeks prior to commencement of the exposure experiments to allow for acclimatization. Prior to and during the experiments all frogs were housed individually under clean and controlled laboratory conditions, fed *ad libitum*, and observed daily by an experienced animal handler and/or veterinarian for health status and clinical signs of disease. Full methodological details for both tissue-response and survival experiments are presented by Grogan *et al.* (2018) (also see Bataille *et al.* 2015 and Grogan 2014).

Exposure experiment

Frogs were confirmed negative to Bd prior to the commencement of the experiments via qPCR (see below). The tissue-response experiment consisted of 18 frogs from each of Eucumbene and Kiandra populations (including 6 negative control animals from each population), and 15 frogs from Grey Mare (including 3 negative control animals; Table 3). These frogs were sourced from Kiandra clutch B, Eucumbene clutch D and Grey Mare clutch B (see Grogan *et al.* 2018). A Bd strain isolated nearby approximately two years before was used for inoculations (AbercrombieNP-*L.booroolongensis*-09-LB-P7), being maintained as described previously (Cashins *et al.* 2013). Thirty-six experimental animals in the tissue response experiment and 278 frogs in the survival experiment were individually exposed to 750,000 zoospores in 25ml dilute salts solution (DSS). Negative control group frogs were treated similarly, but were sham exposed with only DSS. Details of the survival experiment exposure are described by Grogan *et al.* (2018). Animal experiments were approved by James Cook University Animal Ethics Committee (A1589), and were performed in accordance with the welfare requirements of the funding grant provided by Morris Animal Foundation.

Euthanasia, sampling and determining infection intensity via qPCR

A randomized block design was used to select 17 frogs (allocated amongst populations and treatment groups) for each of three sampling sessions (performed at 4, 8 and 14 DPE corresponding with subclinical infections). Immediately prior to euthanasia, frogs were swabbed to confirm infection status and quantify Bd infection intensity via qPCR, and mass and snout-urostyle length were recorded. Frogs were then humanely euthanized via double

pithing, and a midline coeliotomy was performed for tissue collection. Tissues collected included ventral abdominal and thigh skin, liver and spleen, and these were immediately transferred to RNAlater (Qiagen) and refrigerated overnight at 4 °C before being stored longer-term at -80 ºC. Gender was ascertained via examination of coelomic reproductive organs and forelimb nuptial pads on males. In brief, for the concurrent survival experiment, frogs were observed daily and euthanized when they demonstrated clinical signs of disease (described in detail by Grogan *et al.* 2018). Bd infection intensity data (in zoospore equivalents, ZSE) was collected via swabbing with a sterile dry swab, which was then stored dry at 4 °C before being analyzed for Bd DNA with the TaqMan real-time qPCR protocol (following Garland *et al.* 2009; Hyatt *et al.* 2007). Individual swabs were analyzed in triplicate and each run included an internal positive control.

RNA extractions and Illumina sequencing

Total RNA was isolated from skin, liver and spleen tissue samples following the manufacturer protocols for 5-Prime PerfectPure RNA Tissue kits for liver and skin samples and Qiagen RNeasy mini kits for spleen samples (the spleens were considerably smaller in volume), as described by Grogan *et al.* (2018). RNAstable plates (Biomatrica) were used to ship total RNA samples dry and at room temperature. Total RNA quality and quantity were determined via (1) Nanodrop 1000 (Thermo, DE, USA) spectrophotometer, (2) fluorimetric RiboGreen assay (Thermo, DE, USA), and (3) capillary electrophoresis with Agilent BioAnalyzer 2100 (Agilent Technologies, CA, USA). Samples containing > 1 ug total RNA and having an RNA Integrity Number (RIN) > 8 passed quality control. Library preparation and sequencing were performed at the Minnesota BioMedical Genomics Centre, USA. Up to 12 samples were multiplexed on each flow cell lane, and sequencing was performed with the Illumina HiSeq 2000 (Illumina, San Diego, CA) generating > 10 million 100 bp paired-end reads for each sample. Base call data were de-multiplexed with CASAVA software 1.8.2 (Illumina, San Diego, CA), generating .fastq files for each sample (Grogan *et al.* 2018).

Data preparation, transcriptome assembly and functional annotation

Sequence reads from each sample were examined for read quality using FastQC. Trimmomatic 0.30 (Bolger *et al.* 2014) was used to trim adapter sequences, crop random hexamers (Hansen *et al.* 2010), perform sliding window trimming (window size 4, required quality 15), trim flanking low quality bases, and remove reads with length < 75 bases, while retaining widowed reads. Digital normalization (DigiNorm; Brown *et al.* 2012) was used to remove read redundancy, and Bowtie (Langmead *et al.* 2009) removed reads aligning to the Bd genome. We then generated *de novo* tissue-specific transcriptome assemblies with Trinity (Haas *et al.* 2013; tissue-specific for logistical reasons). To reduce partial or erroneous contigs, we mapped reads back to the assembly and removed contigs with < 4 reads per million mappable reads (Harrison *et al.* 2012; Moghadam *et al.* 2013). Identification of the protein coding regions in the assembled transcripts was performed using TransDecoder (Trinity). We then used BLAST2GO version 3.3 (Conesa *et al.* 2005), with basic linear alignment search tool (BLASTx) to assign sequences to an in-house anuran database consisting of the Amphibia subset of the National Center for Biotechnology Information (NCBI) non-redundant protein database. We functionally annotated each assembled transcript (gene) via BLAST2GO with data from the Gene Ontology [GO] consortium, Enzyme Code and Inter Pro (Jones *et al.* 2014) databases (detailed by Grogan *et al.* 2018). For the purposes of downstream interpretations, we considered BLASTx annotations with a minimum eValue of $\leq 1x10^{-3}$ and mean sequence similarity $\geq 40\%$.

Statistical analysis - differential gene expression, clustering and GO enrichment analyses

The R package RSEM (Li & Dewey 2011) was used to quantify the abundance of genes and isoforms in individual frog tissue samples in combination with the above-described tissue-specific assembled transcriptomes, generating tables of transcript count data. The data for the three populations and three tissue types were analysed independently. EdgeR from the Bioconductor suite (Robinson *et al.* 2010) was then used to identify statistically differentially expressed genes between experimental groups (independently for the various within-population comparisons), using raw gene read counts as recommended. Significantly dysregulated transcripts were identified as those with FDR < 0.05 using Benjamini-Hochberg multiple testing correction. We first compared the within-population pooled unexposed control frog samples with respective exposed frog samples taken at 4, 8 and 14 DPE within

the three populations, to identify genes that were either up- or down-regulated relative to the control baseline of homeostatic gene expression. We then performed GO term enrichment analysis (using Fisher's exact test and FDR < 0.05) on these sets of genes identified as differentially expressed from each time comparison in order to determine enriched functional profiles. We used the fully annotated tissue-specific transcriptomes as the reference sets for these analyses. As a quality control measure, we performed batch effect analysis on unexposed control frog samples from the three tissue types to identify any underlying systematic differences between sampling sessions (Supplementary Note S1, Fig. S1).

In a separate analysis, we performed Euclidean distance clustering to identify broad expression patterns of differentially expressed genes (categorized by population within tissue type), incorporating genes with FDR < 0.05 and $\log_2$ fold-change ($\log_2$FC) > 1 (using Trinity and custom scripts). After manual selection of major clusters, we plotted heatmaps with individual frog samples (columns of the heatmaps) ordered by increasing infection intensity within sampling period groups in time-series fashion ('heatmap.3' from R package GMD; Zhao & Sandelin 2012). We similarly performed GO functional enrichment analysis on the resulting cluster groups (plus the full set of genes from all clusters), as above, against the respective tissue-specific transcriptome reference set.

In order to specifically examine the expression of immune-associated genes, we manually extracted and curated a list of differentially expressed genes with putative immune functions for each population and sampling session. For this list, we searched for an *a priori* defined list of terms related to expected immune functions from among annotations for each gene (derived from the BLASTx gene name/description and GO terms).

RESULTS

Experimental results

All 51 alpine tree frogs survived the duration of the tissue response experiment (up to 14 DPE) without demonstrating clinical signs of chytridiomycosis (muscle weakness, lethargy, peripheral erythema or inability to maintain normal upright posture). Demographic data on the sampled frogs including infection intensities assessed via qPCR pre-euthanasia at time of

sampling are listed in Table 1. Unexposed control group frogs remained uninfected for the duration of the experiment except for one indeterminate result (one well positive, < 2 zoospore equivalents, ZSE [Lva010 from Kiandra sampled at 8 DPE]). Exposed frogs became infected (consistently testing positive except one indeterminate result [Lva399 from Kiandra sampled at 4 DPE] and one negative result [Lva076 from Grey Mare sampled at 8 DPE]), demonstrating variable but increasing Bd intensities through time. Mean capped intensities (when the results curve was truncated corresponding to the highest qPCR standard) were 34, 2,200 and 11,161 ZSE for 4, 8 and 14 DPE respectively (without truncating for the highest qPCR standard the 14 DPE average increased to 21,482 ZSE). These infection intensities are comparable to those observed from wild alpine tree frogs (Scheele *et al.* 2015). Frogs from different populations did not differ significantly in their mean mass or snout-urostyle length (SUL) (one-way ANOVA not assuming equal variances, $F = 0.938$, $p = 0.398$, 2 df for mean mass; $F = 2.423$, $p = 0.099$, 2 df for SUL). However, we detected a significant difference in log-transformed uncapped Bd infection intensities between exposed frogs from the three populations at 14 DPE with samples from long-exposed Kiandra demonstrating the lowest intensities ($F = 6.5924$, $p = 0.044$, 2 df for $\log_{10}[ZSE+1]$; Table 1). In addition, an observable (but non-significant) trend indicated lower infection intensities throughout the three sampling sessions in frogs from the Kiandra population (Fig. 1).

In the concurrent large survival experiment using other animals from these and additional clutches (Bataille *et al.* 2015; Grogan 2014; Grogan *et al.* 2018), all frogs from the respective clutches died by 86 DPE except for one frog from Kiandra. However, mean survival time for frogs from Kiandra was greater than from populations Grey Mare and Eucumbene (Fig. 2). Frogs from Kiandra (Clutch B; N = 20; mean time to death for the 19 that died = 36 days) survived for significantly longer when compared with the other long-exposed population Eucumbene (Clutch D; N = 19; mean time to death = 28 days; $\chi^2 = 19$, df = 1, $p < 0.0001$; using the Mantel-Haenszel test; Harrington & Fleming 1982), and the naïve population Grey Mare (Clutch B; N = 20; mean time to death = 27 days; $\chi^2 = 29.9$, df = 1, $p < 0.0001$). However, there was no evidence for a significant difference in time to death between frogs from Eucumbene and Grey Mare ($\chi^2 = 0.7$, df = 1, $p = 0.41$). Comprehensive raw data records for both these experiments are presented by Grogan *et al.* (2018) (also see Bataille *et al.* 2015 and Grogan 2014).

RNA-seq data, transcriptome assembly and annotation

Total RNA was successfully extracted from all 152 skin, liver and spleen tissue samples collected from frogs. The amount of total RNA extracted varied by tissue type and size; mean total RNA extracted was 81.27 ug for liver samples (SD 45.58 ug; N = 51), 19.76 ug for skin samples (SD 8.51 ug; N = 51), and 5.47 ug for spleen samples (SD 1.69 ug; N = 50). Of these samples, 148 passed quality control with a quantity > 1 ug, and RIN > 8. Shipping at room temperature using RNAstable plates did not adversely impact RNA quality or resuspended mass. All 16 Illumina HiSeq 2000 flow cell lanes generated > 160 million pass filter reads (> 10 million reads per sample). Average number of raw reads per sample for liver was 15,819,807, SD 1,940,924, N = 50; for skin was 15,220,337, SD 4,778,641, N = 51; for spleen was 16,997,724, SD 2,302,778, N = 50; and overall total number of reads = 2,417,113,729. Phred quality scores were high within individual reads and across the data set (average Q-Score = 34.7; 99.9-99.99% base call accuracy). Trinity transcriptomes were assembled *de novo* for each tissue, yielding 21,269 Trinity 'transcript clusters' (hereafter referred to as genes) for liver; 26,894 genes for skin; and 28,879 genes for spleen tissues (Supplementary Table S1). These gene numbers are comparable with similar non-model amphibian species' *de novo* transcriptome assemblies (Ellison *et al.* 2015). Approximately two thirds of assembled genes were annotated with at least one significant hit via BLASTx against the anuran non-redundant protein database (69.6% of total assembled genes from liver tissues, 66.7% skin, 64.9% spleen), and full gene ontology (GO) annotations were assigned to marginally fewer (57.3% of total assembled genes from liver tissues, 54.4% skin, 52.5% spleen).

General differential gene expression trends

Comparison of gene expression levels between negative control (uninfected) and exposed frog groups revealed distinct grouping by population for all three tissue types using multi-dimensional scaling plots (Robinson *et al.* 2010) (Fig. 3). Comparing exposed with control samples on a time-series basis (samples from 4, 8 and 14 DPE versus controls within population and tissue type groups), revealed the highest numbers of differentially expressed

genes at the late subclinical infection time point (14 DPE) particularly in skin samples (Fig. 4, Supplementary Tables S2-S4). In addition, we observed a trend of decreasing gene dysregulation in the skin samples at 14 DPE in frogs from Grey Mare, Eucumbene and Kiandra respectively. The range of gene expression fold change [log_2FC] values varied between approximately 13 (up-regulated relative to controls) and -13 (down-regulated) for all differentially expressed genes from all tissue types (Supplementary Tables S2-4).

We found little overlap of differentially expressed genes between populations (with control samples taken as baseline) in both the liver and spleen tissues, with greatest number of genes shared between the two long-exposed populations Eucumbene and Kiandra (Figs. 5a and 5c; Micallef & Rodgers 2014). However, many differentially expressed genes were found to be shared between populations in the skin samples, particularly between samples from the two most susceptible populations Grey Mare and Eucumbene (total of 1055 genes shared between Grey Mare and Eucumbene samples; Fig. 5b). Venn diagrams for differentially expressed genes that were shared between populations separated by sampling time post exposure can be found in Supplementary Figs. S2-S4.

Clustering and gene ontology enrichment analysis

We identified 2-9 gene expression clusters for each tissue-population combination, and cluster expression patterns were most distinct in skin samples from Eucumbene and Grey Mare (Figs. 6a and 6b). Heatmaps and cluster group fold-change averages (Fig. 6, Table 2, and Supplementary Fig. S5 and Table S5) revealed a gradually increasing time-series trend in gene expression in Eucumbene and Grey Mare clusters SkEuc1 and SkGre2, and a correspondingly decreasing trend in SkEuc2 and SkGre1 (Figs. 6a, 6b, and Table 2). A more distinct jump in expression was observed for skin samples from Kiandra, whereby expression of genes in SkKia5 increased and SkKia4 decreased at 4 DPE relative to controls (SkKia1, SkKia2 and SkKia3 contained relatively few genes; Fig. 6c and Table 2). This occurred despite one frog sampled in the 4 DPE group recording only a low and indeterminantly positive infection intensity (Lva399).

GO enrichment analysis on major skin clusters increasing expression through time from the three populations (SkEuc1, SkGre2 and SkKia5) revealed significant over-representation of a relatively large group of immune-associated processes together with terms related to collagen metabolism, ion transport, molecule biosynthesis, and a variety of degenerative and salvage pathways (Fig. 6, Supplementary Fig. S5, Table S6). Significantly enriched immune-associated GO biological process terms in these clusters included for example 'defense response', 'inflammatory response', 'immune response' (Supplementary Fig. S5 and Table S6). In contrast, immune-related processes were not represented in the main clusters with decreasing expression through time post exposure (SkEuc2, SkGre1, SkKia4). Other major groups of GO process terms were associated with epithelial homeostasis, water and ion transport and homeostasis, and musculoskeletal system processes. Significantly enriched GO biological process terms included for example 'intercellular transport', 'intracellular transport', 'cellular water homeostasis' and 'muscle contraction' (Supplementary Table S6).

Although expression patterns were generally less clear in liver and spleen samples, significantly enriched immune-associated GO biological process terms were found in clusters that demonstrated a trend of increasing expression with time post exposure (LiEuc2, LiKia4, SpEuc2 and SpEuc5). However, unexpectedly, immune-associated terms were also significantly enriched in LiEuc1 (low expression at 14 DPE), LiGre1 (peak in expression at 8 DPE), LiKia1 (low expression at 4 DPE) and SpEuc3 (low expression at 14 DPE) (Supplementary Fig. S5).

Differential expression of immune-associated genes

Functional annotation of the differentially expressed gene lists (Supplementary Tables S2-S4) revealed many genes with putative annotations related to the immune response (80 unique genes in liver, 629 in skin, and 159 in spleen samples using our search term list; Fig. 7 and Supplementary Tables S7-S9). Gene functional homologies to all major recognized components of both the innate and adaptive vertebrate immune systems were identified. Genes associated with B and T lymphocytes including immunoglobulins (Igs), MHC, Fc receptors and NF-κB were dysregulated in exposed frogs. Genes associated with the classical, alternative and lectin complement pathways as well as lysozyme were found differentially

expressed. We also identified many dysregulated genes related to antigen-presenting, phagocytic, and cytotoxic cells including macrophages and neutrophils, as well as major groups of pattern recognition receptors including toll-like and mannose-receptors. There were also many examples of differentially expressed eicosanoid inflammatory mediators including leukotrienes, nitric oxide, as well as cytokines and chemokines including interferons (IFNs), interleukins (ILs), and tumor necrosis factors (TNFs). Log_2FC values for immune-associated genes varied from -8.6 to 7.8 for liver, from -10.1 to 9.0 for skin, and -8.9 to 10.2 for spleen samples (Supplementary Tables S7-S9).

Similarly to general gene expression trends, greatest numbers of immune-associated genes were expressed at the late subclinical infection time point (14 DPE) particularly in skin samples, with a similar trend observed of decreasing gene dysregulation in frogs from Grey Mare, Eucumbene and Kiandra respectively (Fig. 7). Many more immune-associated genes were found to be up-regulated than down-regulated when compared with unexposed control frogs (approximately three to four times; for example, 671 up-regulated compared with 200 down-regulated immune-associated genes in the skin, Fig. 7), and at least in the skin tissues, most of these down-regulated genes were only distantly functionally related to immune processes (Supplementary Table S7-S9). Of particular note, however, a comparatively large number of T-cell associated genes were identified as down-regulated in the skin of Grey Mare frog samples at 14 DPE, and the skin and spleen of Eucumbene frog samples at 14 DPE (Fig. 7).

Of interest, the immune-associated genes with highest log_2FC values in the skin (highly up-regulated compared with controls; $log_2FC > 4$) were found predominantly in the two more susceptible populations, Eucumbene and Grey Mare at 14 DPE (60 genes). The most highly up-regulated of these included heat shock proteins (log_2FC 9.0), IFN-induced genes (IFN-induced very large GTPase 1-like [log_2FC 8.8 and 7.8]), and antigen presentation genes (log_2FC 8.7). Contrastingly, Kiandra frogs demonstrated marked up-regulation only of MHC class II alpha chain genes in the skin at all time points post exposure [log_2FC 6.3, 6.2 and 5.9].

Differential expression of immune-associated genes in early subclinical infection associated with lower infection intensities and improved survival

Frogs from Kiandra demonstrated a broader representation of dysregulated immune-associated genes than frogs from the other two populations at 4 DPE (see Supplementary Note S2 for details). These included up-regulated genes (predominantly in skin samples) associated with antigen processing and presentation (MHC class II), cytokines (TNF, IL), members of the alternative complement pathway (factor B and a c3b analogue), the humoral immune response (Igs), and general inflammation and wound healing processes. T-cell differentiation genes and IFN associated GTPase genes were down-regulated in all three tissues (for example, IFN-induced very large GTPase [log_2FC -7.3] in the liver). Contrastingly, frogs from Grey Mare demonstrated marked up-regulation of these IFN-induced GTPases in all three tissues at 4 DPE (ie, [log_2FC 8.8] in skin) (interestingly, these genes were also up-regulated at 8 and 14 DPE). Otherwise, frogs from Grey Mare and Eucumbene exhibited minimal early immune response to Bd infection compared with Kiandra. Some antigen processing genes and cytokines were upregulated in the skin of Grey Mare frogs, while Eucumbene frogs had a strong early alternative complement pathway response in the liver.

Only a mild immune response was observed across tissues from Eucumbene and Kiandra frogs at the mid-subclinical infection time point (8 DPE), with up-regulated genes including antigen processing and presentation genes and cytokines from both populations, and alternative complement pathway and immunoglobulins from Kiandra frogs. Complement pathways were contrastingly down-regulated in the skin and spleen of frogs from Eucumbene at 8 DPE. Frogs from Grey Mare demonstrated a comparatively more substantial immune response at 8 DPE, including up-regulated genes associated with antigen processing and presentation (MHC) and IFNs (total of 26 unique immune-associated genes identified in the skin samples).

DISCUSSION

Frogs from a long-exposed population (Kiandra) of the alpine tree frog (*Litoria verreauxii alpina*) with a more disease-resistant phenotype displayed a more robust early (4 days post exposure; DPE) immune response at the level of gene expression in comparison with a

susceptible Bd-naïve population (Grey Mare), and a susceptible long-exposed population (Eucumbene). Components of this early immune response may be vital for conferring chytridiomycosis resistance. Although the more susceptible populations exhibited larger immune responses at the late subclinical stage of infection (14 DPE), this finding is consistent with previous studies and suggests this late-stage response was non-protective (Ellison *et al.* 2014; Ellison *et al.* 2015).

In our experiment we investigated infection intensities as well as functional immune response to subclinical chytridiomycosis (at 4, 8 and 14 DPE) at the site of infection (skin), and in two immune-related organs (spleen and liver). Frogs from Kiandra demonstrated a trend of lower infection intensities as early as 4 DPE onwards (significant at 14 DPE) when compared with frogs from the other two populations suggesting their early manifestation of clinically protective resistance (Fig. 1). Protective immune responses in amphibians are usually activated early in the infection process. For example, pathogen-induced antibodies to Frog Virus 3 were reported at one week post-exposure and cell-mediated infection clearance occurred within 2-3 weeks (Gantress *et al.* 2003; Robert *et al.* 2005). Frogs from Kiandra demonstrated a more robust immune response in early stage infection compared with the two more susceptible populations. Immune-associated genes that were up-regulated relative to controls in the skin of frogs from Kiandra included representatives of both functioning innate and adaptive immune systems (antigen processing and presentation genes, cytokines, alternative complement pathway genes, immunoglobulins, genes related to the humoral immune response, and general inflammatory genes). However, there was some early evidence for the down-regulation of T-cell differentiation genes and IFN-induced GTPase genes.

Overall, the baseline transcriptional response was divergent between the three populations, and although untested, this could be a result of long-term geographic isolation accompanied by a degree of parapatric speciation (Figs. 3-5; Gavrilets *et al.* 2000). As expected from previous studies (Ellison *et al.* 2014; Ellison *et al.* 2015; Rosenblum *et al.* 2009) our gene expression results from the late subclinical infection stage (14 DPE) were the most highly dysregulated, particularly so in skin samples. However, the trend in the numbers of dysregulated genes at 14 DPE was negatively associated with survival and infection intensity results among populations. Skin samples from Grey Mare, the Bd-naïve and most susceptible

population, demonstrated the highest number of differentially expressed genes at the late subclinical time point with the greatest number of dysregulated immune-associated genes (Fig. 7). In contrast, skin samples from Kiandra, the most resistant and one of the long-exposed populations, demonstrated the lowest level of differentially expressed genes (including immune-associated genes) at 14 DPE. These findings are consistent with the results from Ellison *et al.* (2015) where more susceptible species were found to have a more dysregulated immune response than resistant species at a later stage of infection. Indeed, Ellison *et al.* (2014) found a marked transcriptional response of immune-associated genes in moribund frogs even in the highly susceptible species, *Atelopus zeteki*. We speculate that the observed highly dysregulated gene expression at 14 DPE, particularly in highly infected Grey Mare and Eucumbene populations, may either represent immunopathology (a dysregulated and damaging immune response), or a protective response to marked epithelial disruption. Epidermal damage occurs as Bd burdens increase and includes erosions, micro-vesicles, and less frequently ulcerations and bacterial infections that may be associated with cellular inflammation (Berger *et al.* 2005b; Brutyn *et al.* 2012).

Dysregulated genes with functional homology to all major components of the vertebrate immune system were identified by gene ontological annotation of our tissue transcriptomes. The majority of these genes were up-regulated in skin samples from the late subclinical stage of infection in the most susceptible populations Grey Mare and Eucumbene (Fig. 7). A correspondingly broad range of immune-associated GO biological process terms was identified from skin samples in association with distinct gene clusters that exhibited increased expression with time post exposure. Notably, where heatmaps revealed a gradual increase in gene expression in these clusters from Grey Mare (SkGre2) and Eucumbene (SkEuc1), the corresponding cluster from Kiandra (SkKia5) increased more noticeably from 4 DPE indicating an earlier immune response to Bd consistent with our trend of lower infection intensities and improved survival times (Fig. 6, Table 2, Supplementary Fig. S5 and Table S6).

Skin clusters that exhibited decreased expression with time post exposure from all three populations were significantly enriched for predominantly homeostatic mechanisms, water and ion transport, musculoskeletal system processes and cardiovascular system processes

related to conduction, contraction and regulation of heart rate (Supplementary Fig. S5 and Table S6). These findings likely constitute essential mechanisms underlying the observed late stage clinical signs of chytridiomycosis which include skin ulceration and sloughing, ion loss, dehydration, lethargy and bradycardia, ultimately leading to asystolic cardiac arrest and mortality (Voyles *et al.* 2012; Voyles *et al.* 2009). Cluster expression patterns from liver and spleen tissues were much less distinct in all three populations, with more clusters identified, and fewer significantly enriched GO terms. While some liver and spleen clusters with increasing expression through time also demonstrated significant enrichment for immune-associated GO terms, several other clusters with immune terms exhibited peaks or dips in expression at various time-points post exposure, indicating that immune gene expression is comprised of a complex and dynamic network of immune signals varying between tissues over time.

Interestingly, we observed the down-regulation of many lymphocyte-associated (particularly T-cell related) genes in the skin samples of infected Grey Mare frogs at 14 DPE, and the skin and spleen of infected Eucumbene frogs at 14 DPE (Fig. 7). One spleen sample cluster (SpEuc3) that exhibited decreased expression over time was significantly enriched for numerous T-cell associated processes (Supplementary Fig. S5g). There was also some evidence for T-cell suppression in frogs from Kiandra. These findings are consistent with the results of Ellison *et al.* (2014) and previous findings of *in vitro* lymphocyte suppression mediated by a putative Bd-secreted virulence factor (Fites *et al.* 2013). T-cell associated cell-mediated immunity is likely to be especially important for intracellular pathogens such as Bd (Rollins-Smith *et al.* 2009), and involves differentiation of T lymphocytes into cytotoxic T-cells which recognise and stimulate apoptosis of infected host cells, or phagocytosis by cells of the innate immune system. Down-regulation of T-cell associated genes likely cripples the longer-term amphibian adaptive immune response to chytridiomycosis, despite an otherwise highly up-regulated immune system. Our result is also consistent with 1) the lack of cellular inflammation around sites of Bd infection (Berger *et al.* 2005b), and 2) reinfection experiments where highly effective adaptive immunity was not demonstrated in the species tested (Cashins *et al.* 2013; McMahon *et al.* 2014). We speculate that although frogs from the Kiandra population demonstrated a robust early immune response to Bd, the efficacy of cell-mediated immunity may have been stifled by Bd-associated suppression of the adaptive

590 immune system, preventing resolution of infection in the longer term (in the survival study all
591 but one of the frogs from Kiandra Clutch B died by 86 days post exposure although they
592 survived on average longer than frogs from the other two populations) (Bataille *et al.* 2015;
593 Grogan 2014).
594
595 Of particular interest, down-stream processes of IFN were down-regulated in all three tissues
596 of frogs from Kiandra at 4 DPE. This finding is in direct contrast to the marked up-regulation
597 of IFN-induced genes in all three tissues of Grey Mare frogs throughout infection [several
598 genes with $\log_2$FC > 5], and the study by Price *et al.* (2015) where 11 of 29 annotated up-
599 regulated transcripts in liver samples from the Bd vs control comparison at 4 DPE represented
600 similar IFN-induced genes. Frogs from Eucumbene demonstrated no such clear signal. IFN-γ
601 is of central importance for non-specific macrophage-associated cell-mediated immunity,
602 although it may also be involved with antibody-associated cytotoxicity and has been linked
603 with some autoimmune processes (Farrar & Schreiber 1993). Interferon-induced GTPases
604 play an important role in autonomous somatic cell immunity and may promote autophagy of
605 intracellular microbial pathogens (Kim *et al.* 2012). The marked early up-regulation of IFN-
606 induced pathways (this study and Price *et al.* 2015) in conjunction with lymphocyte
607 suppression and clinical evidence of susceptibility in frogs from Grey Mare suggests that 1)
608 these responses are mis-directed and insufficiently protective against Bd, and 2) these
609 pathways may play a more fundamental role in pathogenesis. Otherwise, frogs from Grey
610 Mare exhibited only mild evidence of an early immune response to Bd infection compared
611 with those from Kiandra, while frogs from Eucumbene demonstrated an early classical
612 complement response in the liver (Supplementary Note S2 and Tables S7-S9).
613
614 In the concurrent clinical survival study (Bataille *et al.* 2015; Grogan 2014; Grogan *et al.*
615 2018), frogs from long-exposed Kiandra (including those from Clutch B) survived
616 significantly longer than frogs from the two other populations (Fig. 2), which may be
617 consistent with the evolution of resistance in frogs from Kiandra over approximately 20 years
618 of intergenerational exposure to Bd. Interestingly, the Eucumbene population was also long-
619 exposed, however frogs from Eucumbene were found to be comparatively susceptible to Bd.
620 We acknowledge the caveat of working with a small number of populations, which was
621 necessary for logistic feasibility. We also acknowledge the lack of replication of our naïve

population, a limitation that was beyond our control, but that potentially confounds infection history with unidentified causes of population variation in immunity. However, these caveats do not negate the value of our study because our findings relate the degree of observed clinical resistance to the underlying transcriptomic responses of the respective populations, rather than relying on long-term infection history as the explanatory factor.

An accompanying field study (Scheele *et al.* 2015) suggests that a likely mechanism for continued persistence of these populations despite high Bd-associated adult mortality is high compensating recruitment. Scheele *et al.* (2015) found a predominance of two year old adults in the long-exposed populations, indicating that the majority of adults die during their first breeding season. Behavioural and life-history characteristics of juvenile *L. v. alpina* mean that frogs don't commonly become infected prior to returning to the pond to breed. If adults typically breed successfully prior to succumbing to chytridiomycosis, this may reduce the selection pressure acting on disease resistance traits, resulting in poor evolution of immunity in this species.

This is the first study to identify underlying immune mechanisms at the early subclinical stage of infection that may be related to evolved resistance to Bd. Multiple lines of evidence demonstrated that a more resistant amphibian phenotype from an evolutionarily long-exposed population, had an early immune response at the level of gene expression which likely explains the reduced early Bd infection intensities and extended survival. Additionally, our results were consistent with Bd-associated lymphocyte suppression, and raise questions about the role of IFN-induced pathways in Bd pathogenesis. We recommend future studies target pathways involved in cell-mediated immunity to elucidate the mechanisms underlying early responses to infection, the role of cytokines such as IFN-γ and host-mediated T-cell suppression.

ACKNOWLEDGEMENTS

We thank E. Rosenblum and L. Rollins-Smith for advice on study design, and R. Speare for initiating this collaboration. We thank R. Spindler and members of the Taronga Zoo Herpetofauna Department for assistance with logistics for the clinical experiment and species'

insights. This study was conducted with approval by the James Cook University Animal Ethics Committee (Certificate no. A1589) and Scientific License number: S12848 (D. Hunter). This work was jointly funded by Morris Animal Foundation, US Fish and Wildlife Service - Wildlife Without Borders program, Australian Research Council grants FT100100375, LP110200240 and DP120100811, Taronga Conservation Science Initiative, and NSW Office of Environment and Heritage. The funders had no role in study design, data collection and analysis, decision to publish, or preparation of the manuscript.

REFERENCES

Atkinson CT, Saili KS, Utzurrum RB, Jarvi SI (2013) Experimental evidence for evolved tolerance to Avian Malaria in a wild population of low elevation Hawai'i 'Amakihi (*Hemignathus virens*). *Ecohealth* **10**, 366-375.

Bataille A, Cashins SD, Grogan L, *et al.* (2015) Susceptibility of amphibians to chytridiomycosis is associated with MHC class II conformation. *Proceedings of the Royal Society B-Biological Sciences* **282**, 9.

Berger L, Marantelli G, Skerratt LL, Speare R (2005a) Virulence of the amphibian chytrid fungus *Batrachochytrium dendrobatidis* varies with the strain. *Diseases of Aquatic Organisms* **68**, 47-50.

Berger L, Speare R, Skerratt LF (2005b) Distribution of *Batrachochytrium dendrobatidis* and pathology in the skin of green tree frogs *Litoria caerulea* with severe chytridiomycosis. *Diseases of Aquatic Organisms* **68**, 65-70.

Bolger AM, Lohse M, Usadel B (2014) Trimmomatic: a flexible trimmer for Illumina sequence data. *Bioinformatics* **30**, 2114-2120.

Bonneaud C, Balenger SL, Russell AF, *et al.* (2011) Rapid evolution of disease resistance is accompanied by functional changes in gene expression in a wild bird. *Proceedings of the National Academy of Sciences of the United States of America* **108**, 7866-7871.

Bosch J, Sanchez-Tome E, Fernandez-Loras A, *et al.* (2015) Successful elimination of a lethal wildlife infectious disease in nature. *Biology Letters* **11**, 20150874.

Brown CT, Howe A, Zhang Q, Pyrkosz AB, Brom TH (2012) A reference-free algorithm for computational normalization of shotgun sequencing data. *arXiv e-print*, 1203.4802v1202 [q-bio.GN].

Brutyn M, D'Herde K, Dhaenens M, *et al.* (2012) *Batrachochytrium dendrobatidis* zoospore secretions rapidly disturb intercellular junctions in frog skin. *Fungal Genetics and Biology* **49**, 830-837.

686 Cashins SD, Grogan LF, McFadden M, *et al.* (2013) Prior infection does not improve survival against
687 the amphibian disease chytridiomycosis. *Plos One* **8**, 7.
688 Conesa A, Gotz S, Garcia-Gomez JM, *et al.* (2005) Blast2GO: a universal tool for annotation,
689 visualization and analysis in functional genomics research. *Bioinformatics* **21**, 3674-3676.
690 de Graaf H, Pai S, Burns DA, *et al.* (2015) Co-infection as a confounder for the role of *Clostridium*
691 *difficile* infection in children with diarrhoea: a summary of the literature. *European Journal of*
692 *Clinical Microbiology & Infectious Diseases* **34**, 1281-1287.
693 Ellison AR, Savage AE, DiRenzo GV, *et al.* (2014) Fighting a losing battle: vigorous immune
694 response countered by pathogen suppression of host defenses in the chytridiomycosis-
695 susceptible frog *Atelopus zeteki*. *G3-Genes Genomes Genetics* **4**, 1275-1289.
696 Ellison AR, Tunstall T, DiRenzo GV, *et al.* (2015) More than skin deep: functional genomic basis for
697 resistance to amphibian chytridiomycosis. *Genome Biology and Evolution* **7**, 286-298.
698 Farrar MA, Schreiber RD (1993) The molecular cell biology of interferon-gamma and its receptor.
699 *Annual Review of Immunology* **11**, 571-611.
700 Fisher MC, Garner TWJ, Walker SF (2009) Global emergence of *Batrachochytrium dendrobatidis* and
701 amphibian chytridiomycosis in space, time, and host. *Annual Review of Microbiology* **63**, 291-
702 310.
703 Fites JS, Ramsey JP, Holden WM, *et al.* (2013) The invasive chytrid fungus of amphibians paralyzes
704 lymphocyte responses. *Science* **342**, 366-369.
705 Gantress J, Maniero GD, Cohen N, Robert J (2003) Development and characterization of a model
706 system to study amphibian immune responses to iridoviruses. *Virology* **311**, 254-262.
707 Garland S, Baker A, Phillott AD, Skerratt LF (2009) BSA reduces inhibition in a TaqMan (R) assay
708 for the detection of *Batrachochytrium dendrobatidis*. *Diseases of Aquatic Organisms* **92**, 113-
709 116.
710 Gavrilets S, Li H, Vose MD (2000) Patterns of parapatric speciation. *Evolution* **54**, 1126-1134.
711 Grogan LF (2014) *Understanding Host and Environmental Factors in the Immunology and*
712 *Epidemiology of Chytridiomycosis in Anuran Populations in Australia.* , James Cook
713 University.
714 Grogan LF, Berger L, Rose K, *et al.* (2014) Surveillance for emerging biodiversity diseases of
715 wildlife. *Plos Pathogens* **10**, e1004015.
716 Grogan LF, Mulvenna J, Gummer JPA, *et al.* (2018) Survival, gene and metabolite responses of
717 *Litoria verreauxii alpina* frogs to fungal disease chytridiomycosis. *Scientific Data* **In press**.
718 Haas BJ, Papanicolaou A, Yassour M, *et al.* (2013) *De novo* transcript sequence reconstruction from
719 RNA-seq using the Trinity platform for reference generation and analysis. *Nature Protocols* **8**,
720 1494-1512.

Hansen KD, Brenner SE, Dudoit S (2010) Biases in Illumina transcriptome sequencing caused by random hexamer priming. *Nucleic Acids Research* **38**, 7.

Harrington DP, Fleming TR (1982) A class of rank test procedures for censored survival-data. *Biometrika* **69**, 553-566.

Harrison PW, Mank JE, Wedell N (2012) Incomplete sex chromosome dosage compensation in the indian meal moth, plodia interpunctella, based on de novo transcriptome assembly. *Genome Biology and Evolution* **4**, 1118-1126.

Holden WM, Rollins-Smith LA (2014) Skin bacteria protect newly metamorphosed *Rana sphenocephala* from the emerging fungal pathogen *Batrachochytrium dendrobatidis*. *Integrative and Comparative Biology* **54**, E92-E92.

Huang Y, Zaas AK, Rao A, *et al.* (2011) Temporal dynamics of host molecular responses differentiate symptomatic and asymptomatic *Influenza A* infection. *Plos Genetics* **7**.

Hunter D, Pietsch R, Clemann N, *et al.* (2009) Prevalence of the amphibian chytrid fungus (*Batrachochytrium dendrobatidis*) in the Australian Alps. In: *Report to the Australian Alps Liaison Committee: January 2009*.

Hyatt AD, Boyle DG, Olsen V, *et al.* (2007) Diagnostic assays and sampling protocols for the detection of *Batrachochytrium dendrobatidis*. *Diseases of Aquatic Organisms* **73**, 175-192.

Jones P, Binns D, Chang HY, *et al.* (2014) InterProScan 5: genome-scale protein function classification. *Bioinformatics* **30**, 1236-1240.

Kim BH, Shenoy AR, Kumar P, Bradfield CJ, MacMicking JD (2012) IFN-inducible GTPases in host cell defense. *Cell Host & Microbe* **12**, 432-444.

Kinney VC, Heemeyer JL, Pessier AP, Lannoo MJ (2011) Seasonal pattern of *Batrachochytrium dendrobatidis* infection and mortality in *Lithobates areolatus*: Affirmation of Vredenburg's "10,000 zoospore rule". *Plos One* **6**, 10.

Koprivnikar J, Gibson CH, Redfern JC (2011) Infectious personalities: behavioural syndromes and disease risk in larval amphibians. *Proceedings of the Royal Society B-Biological Sciences* **279**, 1544-1550.

Langmead B, Trapnell C, Pop M, Salzberg SL (2009) Ultrafast and memory-efficient alignment of short DNA sequences to the human genome. *Genome Biology* **10**, 10.

Leeds TD, Silverstein JT, Weber GM, *et al.* (2010) Response to selection for bacterial cold water disease resistance in rainbow trout. *Journal of Animal Science* **88**, 1936-1946.

Li B, Dewey CN (2011) RSEM: accurate transcript quantification from RNA-Seq data with or without a reference genome. *Bmc Bioinformatics* **12**, 16.

McMahon TA, Sears BF, Venesky MD, *et al.* (2014) Amphibians acquire resistance to live and dead fungus overcoming fungal immunosuppression. *Nature* **511**, 224-227.

Meyer D, Thomson G (2001) How selection shapes variation of the human major histocompatibility complex: a review. *Annals of Human Genetics* **65**, 1-26.

Micallef L, Rodgers P (2014) eulerAPE: drawing area-proportional 3-Venn diagrams using ellipses. *Plos One* **9**, 18.

Moghadam HK, Harrison PW, Zachar G, Székely T, Mank JE (2013) The plover neurotranscriptome assembly: Transcriptomic analysis in an ecological model species without a reference genome. *Molecular Ecology Resources* **13**, 696-705.

Murphy KP (2012) *Janeway's Immunobiology*, 8th edn. Garland Science, New York.

Murray KA, Retallick RWR, Puschendorf R, *et al.* (2011) Assessing spatial patterns of disease risk to biodiversity: implications for the management of the amphibian pathogen, *Batrachochytrium dendrobatidis*. *Journal of Applied Ecology* **48**, 163-173.

Murray KA, Skerratt LF (2012) Predicting wild hosts for amphibian chytridiomycosis: integrating host life-history traits with pathogen environmental requirements. *Human and Ecological Risk Assessment* **18**, 200-224.

Murray KA, Skerratt LF, Speare R, McCallum H (2009) Impact and dynamics of disease in species threatened by the amphibian chytrid fungus, *Batrachochytrium dendrobatidis*. *Conservation Biology* **23**, 1242-1252.

Olson DH, Aanensen DM, Ronnenberg KL, *et al.* (2013) Mapping the global emergence of *Batrachochytrium dendrobatidis*, the amphibian chytrid fungus. *Plos One* **8**, 13.

Osborne W, Hunter D, Hollis G (1999) Population declines and range contraction in Australian alpine frogs. In: *Declines and disappearances of Australian frogs* (ed. Campbell A), pp. 145-157. Environment Australia, Canberra ACT.

Pask JD, Cary TL, Rollins-Smith LA (2013) Skin peptides protect juvenile leopard frogs (*Rana pipiens*) against chytridiomycosis. *Journal of Experimental Biology* **216**, 2908-2916.

Phillott AD, Grogan LF, Cashins SD, *et al.* (2013) Chytridiomycosis and seasonal mortality of tropical stream-associated frogs 15 years after introduction of *Batrachochytrium dendrobatidis*. *Conservation Biology* **27**, 1058-1068.

Price SJ, Garner TWJ, Balloux F, *et al.* (2015) A *de novo* assembly of the common frog (*Rana temporaria*) transcriptome and comparison of transcription following exposure to *Ranavirus* and *Batrachochytrium dendrobatidis*. *Plos One* **10**, 23.

Ragimekula N, Varadarajula NN, Mallapuram SP, *et al.* (2013) Marker assisted selection in disease resistance breeding. *Journal of Plant Breeding and Genetics* **1**, 90-109.

Ramsey JP, Reinert LK, Harper LK, Woodhams DC, Rollins-Smith LA (2010) Immune defenses against *Batrachochytrium dendrobatidis*, a fungus linked to global amphibian declines, in the South African Clawed Frog, *Xenopus laevis*. *Infection and Immunity* **78**, 3981-3992.

Ribas L, Li MS, Doddington BJ, *et al.* (2009) Expression profiling the temperature-dependent amphibian response to infection by *Batrachochytrium dendrobatidis*. *Plos One* **4**, Article No.: e8408.

Robert J, Morales H, Buck W, *et al.* (2005) Adaptive immunity and histopathology in frog virus 3-infected *Xenopus*. *Virology* **332**, 667-675.

Robert J, Ohta Y (2009) Comparative and developmental study of the immune system in *Xenopus*. *Developmental Dynamics* **238**, 1249-1270.

Robinson MD, McCarthy DJ, Smyth GK (2010) edgeR: a Bioconductor package for differential expression analysis of digital gene expression data. *Bioinformatics* **26**, 139-140.

Rollins-Smith LA, Ramsey JP, Reinert LK, *et al.* (2009) Immune defenses of *Xenopus laevis* against *Batrachochytrium dendrobatidis*. *Frontiers in Bioscience* **S1**, 68-91.

Rosenblum EB, Poorten TJ, Settles M, Murdoch GK (2012) Only skin deep: shared genetic response to the deadly chytrid fungus in susceptible frog species. *Molecular Ecology* **21**, 3110-3120.

Rosenblum EB, Poorten TJ, Settles M, *et al.* (2009) Genome-wide transcriptional response of *Silurana (Xenopus) tropicalis* to infection with the deadly chytrid fungus. *Plos One* **4**, e6494. doi:6410.1371/journal.pone.0006494.

Rowley JJL, Alford RA (2007) Behaviour of Australian rainforest stream frogs may affect the transmission of chytridiomycosis. *Diseases of Aquatic Organisms* **77**, 1-9.

Savage AE, Zamudio KR (2011) MHC genotypes associate with resistance to a frog-killing fungus. *Proceedings of the National Academy of Sciences of the United States of America* **108**, 16705-16710.

Scheele B, Guarino F, Osborne W, *et al.* (2014a) Decline and re-expansion of an amphibian with high prevalence of chytrid fungus. *Biological Conservation* **170**, 86-91.

Scheele BC, Hunter DA, Banks SC, *et al.* (2016) High adult mortality in disease-challenged frog populations increases vulnerability to drought. *Journal of Animal Ecology* **85**, 1453-1460.

Scheele BC, Hunter DA, Grogan LF, *et al.* (2014b) Interventions for reducing extinction risk in chytridiomycosis-threatened amphibians. *Conservation Biology* **28**, 1195-1205.

Scheele BC, Hunter DA, Skerratt LF, Brannelly LA, Driscoll DA (2015) Low impact of chytridiomycosis on frog recruitment enables persistence in refuges despite high adult mortality. *Biological Conservation* **182**, 36-43.

Scheele BC, Skerratt LF, Grogan LF, *et al.* (2017) After the epidemic: Ongoing declines, stabilizations and recoveries in amphibians afflicted by chytridiomycosis. *Biological Conservation* **206**, 37-46.

Searle CL, Gervasi SS, Hua J, *et al.* (2011) Differential host susceptibility to *Batrachochytrium dendrobatidis*, an emerging amphibian pathogen. *Conservation Biology* **25**, 965-974.

Skerratt LF, Berger L, Clemann N, *et al.* (2016) Priorities for management of chytridiomycosis in Australia: saving frogs from extinction. *Wildlife Research* **43**, 105-120.
Skerratt LF, Berger L, Speare R, *et al.* (2007) Spread of chytridiomycosis has caused the rapid global decline and extinction of frogs. *Ecohealth* **4**, 125-134.
Venesky MD, Mendelson JR, Sears BF, Stiling P, Rohr JR (2012) Selecting for tolerance against pathogens and herbivores to enhance success of reintroduction and translocation. *Conservation Biology* **26**, 586-592.
Voyles J, Vredenburg VT, Tunstall TS, *et al.* (2012) Pathophysiology in mountain yellow-legged frogs (*Rana muscosa*) during a chytridiomycosis outbreak. *Plos One* **7**.
Voyles J, Young S, Berger L, *et al.* (2009) Pathogenesis of chytridiomycosis, a cause of catastrophic amphibian declines. *Science* **326**, 582-585.
Young S, Whitehorn P, Berger L, *et al.* (2014) Defects in host immune function in tree frogs with chronic chytridiomycosis. *Plos One* **9**, 16.
Zhao XB, Sandelin A (2012) GMD: measuring the distance between histograms with applications on high-throughput sequencing reads. *Bioinformatics* **28**, 1164-1165.

DATA ACCESSIBILITY

Raw sequence data (detailed by Grogan *et al.* 2018) are available from the NCBI Sequence Read Archive under the BioProject Accession Number PRJNA356986. *De novo* assembled tissue-specific transcriptomes (separate for skin, liver and spleen) and tables of gene count results, plus all other associated raw data and metadata are available at Dryad (Accession Number: doi: 10.5061/dryad.t1p7c, and detailed by Grogan *et al.* 2018). Additional Supplementary Information supporting aspects of the analysis and presenting expanded results accompanies this paper (Supplementary Notes S1-2, Supplementary Tables S1-11 and Supplementary Figures S1-5).

AUTHOR CONTRIBUTIONS

L.F.G., S.D.C, L.F.S. and L.B. designed research; D.A.H. and B.C.S. provided field knowledge and experience; L.F.G., S.D.C. and D.A.H. collected the amphibians; M.S.McF. and P.H. provided animal husbandry assistance and advice; L.F.G and S.D.C. performed the clinical experiment and collected samples; L.F.G. performed the RNA extractions; L.F.G. and

857 J.M. performed the bioinformatics analyses; all authors discussed interpretation of results;
858 L.F.G. wrote the manuscript draft; all authors revised the manuscript drafts.
859
860 **Conflicting interests:** The authors declare no conflicting interests.

TABLES

Table 1. Demographic characteristics of study subjects (including sample size, treatment group, gender ratios, mean mass pre-euthanasia, mean snout-urostyle length pre-euthanasia and mean and median infection intensity pre-euthanasia).

	Kiandra		Eucumbene		Grey Mare		F value[a]	P value[a]	df[a]
	Exposed	Control	Exposed	Control	Exposed	Control			
Sample size	12	6	12	6	12	3			
Gender[b]	2M, 4F, 6U	2M, 4U	4M, 5F, 3U	5F, 1M	4M, 6F, 2U	1M, 2F			
Mean mass pre-euthanasia	2.99	3.02	3.02	4.05	3.51	3.19	0.938	0.398	2
Mean SUL pre-euthanasia[c]	29.97	30.72	28.80	32.1	32.27	32.03	2.423	0.099	2
Mean ZSE pre-euthanasia[d]	2158.82	0.28	9442.36	0.00	12114.72	0.00	6.592[e]	0.044[e]	2[e]
Median ZSE pre-euthanasia	290.00	0.00	715.00	0.00	910.00	0.00			

[a]Statistics comparing means between populations (pooling exposed and control frog values) using one-way ANOVA, P value and df degrees of freedom; [b]Genders represented by M for males, F for females and U for unknown gender; [c]SUL is snout-urostyle length measured with Vernier callipers; [d]ZSE is zoospore equivalents as measured by qPCR; [e]Statistics refer to $\log_{10}$-transformed uncapped Bd infection intensities ($\log_{10}$[ZSE+1]) between exposed frogs from the three populations at 14 DPE. Other sampling time comparisons were not significant.

Table 2. Summary of mean expression patterns for the genes in each cluster at each time point, and corresponding example significantly enriched GO biological process terms for these clusters, among skin samples (see Supplementary Table S6 for corresponding tables representing results from liver and spleen samples).

873

Cluster[a] ID	Mean centered log_2(fpkm+1) by sample group[b]				No. of genes	No. GO terms (FDR < 0.05)	Example GO biological process terms[c]
	Control	4 days	8 days	14 days			
SkEuc1	-0.60	-0.19	-0.03	1.12	1285	335	Collagen metabolic process; collagen catabolic process; multicellular organism metabolic process; multicellular organism catabolic process
SkEuc2	0.44	0.15	0.13	-0.95	1325	176	Single-organism intercellular transport; intercellular transport; gap junction-mediated intercellular transport; glycerol transport
SkGre1	0.48	0.53	0.01	-0.90	1430	196	Intracellular transport; single-organism intercellular transport; intercellular transport; gap junction-mediated intercellular transport
SkGre2	-0.73	-0.38	0.05	0.88	1861	277	Collagen metabolic process; collagen catabolic process; multicellular organism metabolic process; multicellular organism catabolic process
SkKia1	-2.43	1.80	0.22	1.63	6	0	N/A
SkKia2	0.21	0.39	-0.20	-0.50	216	86	Cellular potassium ion homeostasis; sodium ion export from cell; establishment or maintenance of transmembrane electrochemical gradient; sodium ion export
SkKia3	-0.29	0.45	-0.64	0.63	31	0	N/A
SkKia4	0.52	-0.55	0.13	-0.35	394	9	Peptide cross-linking

Cluster[a] ID	Mean centered log_2(fpkm+1) by sample group[b]				No. of genes	No. GO terms (FDR < 0.05)	Example GO biological process terms[c]
	Control	4 days	8 days	14 days			
SkKia5	-0.68	0.03	0.12	0.87	647	200	Collagen metabolic process; collagen catabolic process; multicellular organism metabolic process; multicellular organism catabolic process

[a]Clusters are defined by Euclidean distance clustering and manually selected using Trinity script `Manually_define_clusters.R` and labelled (see Fig. 6 and Supplementary Fig. S5 for corresponding visual representations); [b]Arithmetic mean of the centered log_2(fpkm+1) expression values grouped by sampling time in days post exposure, from the output of Trinity script `Manually_define_clusters.R` ('Control' group includes all samples from unexposed frogs); [c]Top four most significantly enriched GO Biological Process terms (where applicable) (full list of overrepresented GO terms available in Table S5); [d]N/A indicates that there were no GO Biological Process terms that were significantly enriched with FDR < 0.05 for the respective cluster.

Table 3. Experimental design outlining the number of frogs from each population and treatment group (Bd exposed or unexposed control) sampled at each time point post exposure.

Populations	Exposure – Day 0 Total # exposed (total # control)[a]	Day 4 # exposed sampled (# control sampled)[b]	Day 8 # exposed sampled (# control sampled)[b]	Day 14 # exposed sampled (# control sampled)[b]
Grey Mare (clutch B)	12 (3)	4 (1)	4 (1)	4 (1)

Eucumbene (clutch D)	12 (6)	4 (2)	4 (2)	4 (2)
Kiandra (clutch B)	12 (6)	4 (2)	4 (2)	4 (2)
Total	36 (15)	12 (5)	12 (5)	12 (5)

[a]Total number of unexposed control frogs shown in parentheses; [b]Number of unexposed control frogs sampled shown in parentheses.

887 **FIGURES**

888 **Figure 1.** Box and whisker plot (with data points overlaid) of $\log_{10}$-transformed uncapped Bd
889 infection intensities ($\log_{10}$[ZSE+1]) for all 51 frogs at time of sampling (days post exposure;
890 DPE), by population (using `geom_boxplot` from ggplot2 R package). Data from uninfected
891 control frogs has been plotted as 'zero' DPE (regardless of actual sampling date), for ease of
892 comparison. Box hinges represent first and third quartiles, and middle represents the median.
893 Whiskers extend 1.5 times the inter-quartile range of the hinge. Visually identified group outliers
894 have been labeled with frog ID for ease of comparison (they were not removed from analyses).
895

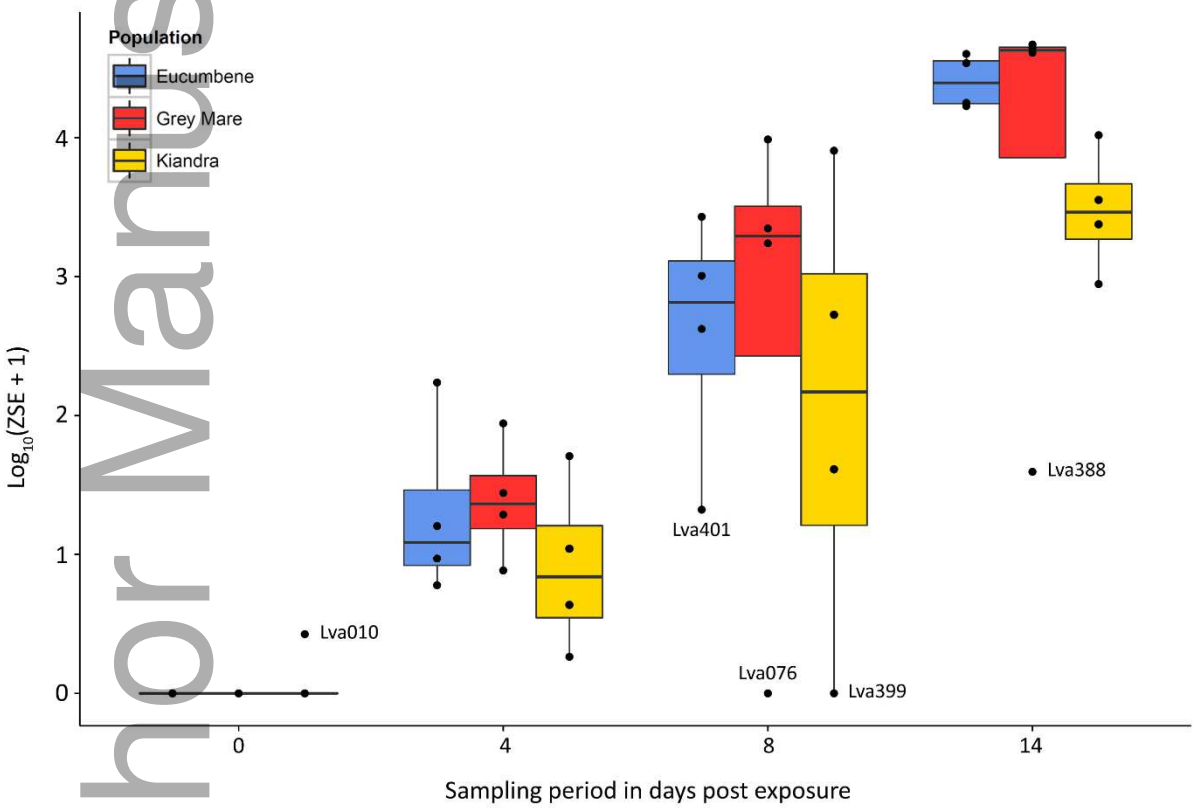

896
897 **Figure 2.** *L.v. alpina* population survival curves by population and clutch for the larger clinical
898 experiment (Bataille *et al.* 2015; Grogan 2014; Grogan *et al.* 2018). These animals were from
899 the same respective clutches as the frogs used in the tissue-response experiment. The horizontal
900 axis indicates survival in days post exposure (the experiment was terminated at 86 DPE for all
901 groups).
902

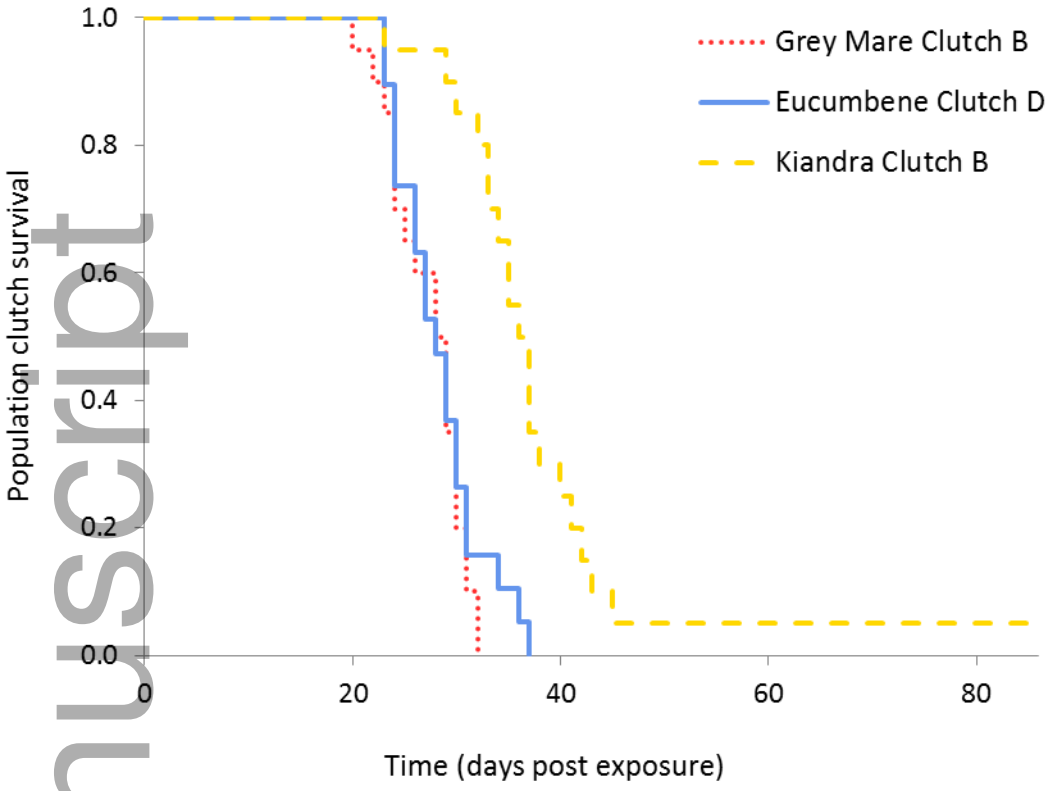

903

904

Figure 3. Unsupervised classical (metric) multi-dimensional scaling plots (using `plotMDS` and recommended settings from the Bioconductor package EdgeR) demonstrating leading log-fold changes between pairs of samples. Uninfected negative control frog samples (▲), Bd-exposed frog samples (●). Samples predominantly cluster by source population (colour groups: Eucumbene, Grey Mare, and Kiandra). (a) Liver samples, (b) skin samples, and (c) spleen samples. Visually identified group outliers have been labeled with frog and tissue ID for ease of comparison (they were not removed from analyses).

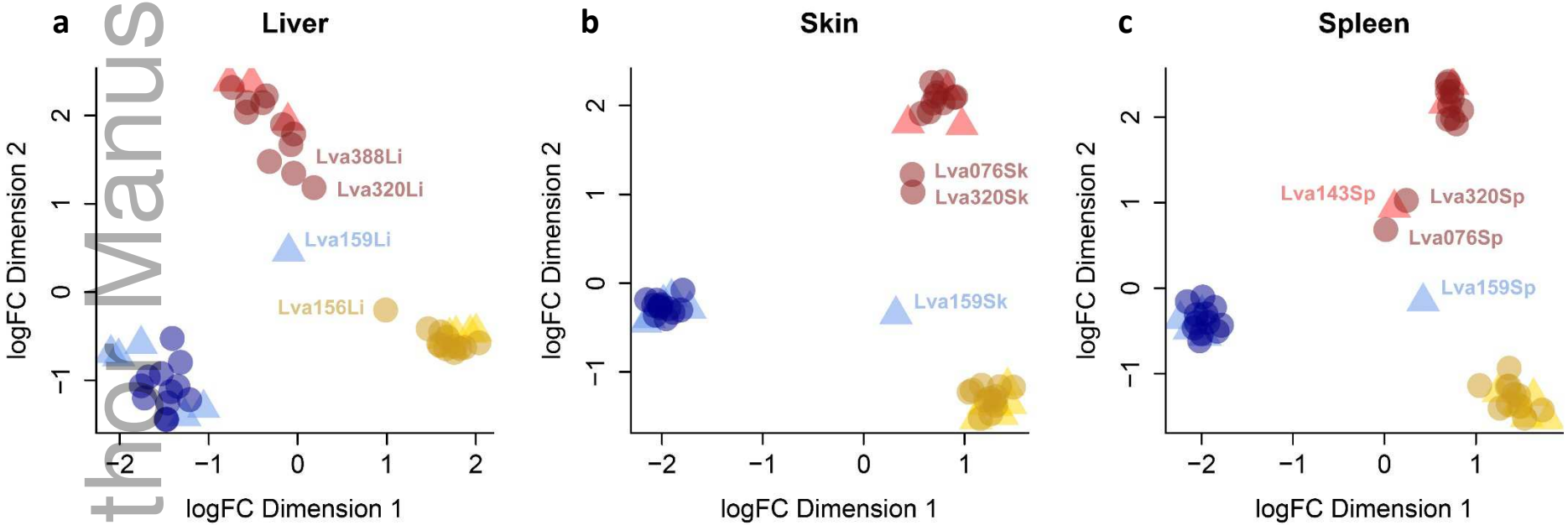

Figure 4. Numbers of up- and down-regulated genes comparing uninfected negative control frog samples and Bd-exposed frog samples within-population at sampling periods post exposure, for all populations and tissues. Gene expression in skin samples from all three populations at 14 DPE were most highly dysregulated.

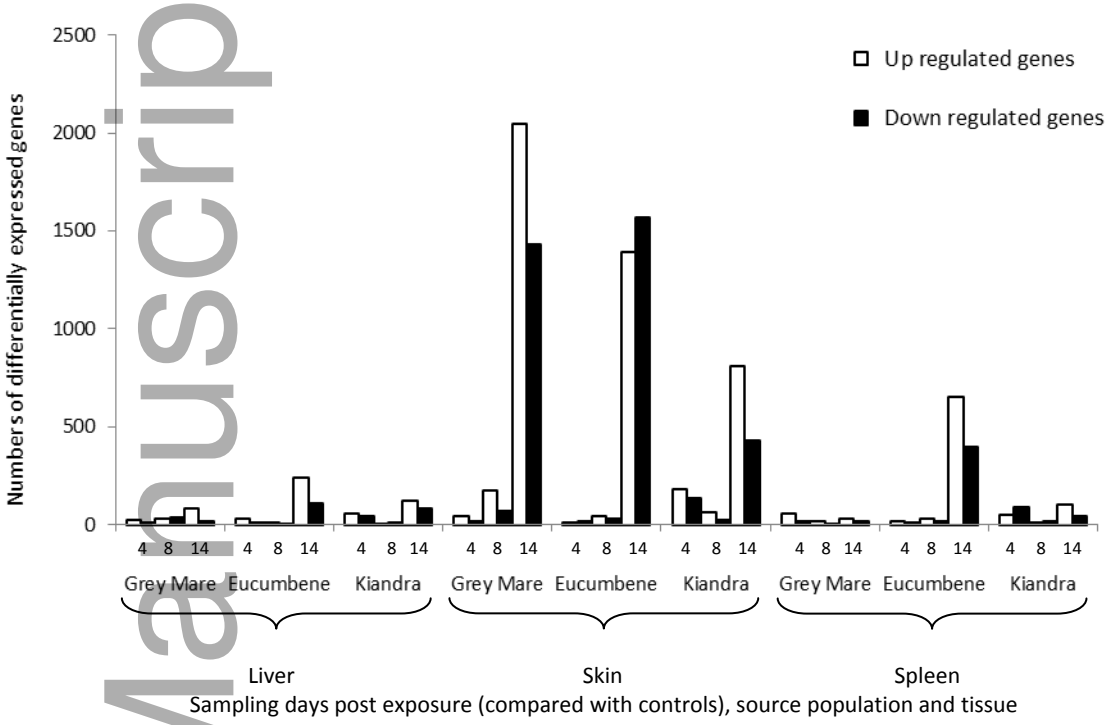

Figure 5. Venn diagrams comparing numbers of genes that were found to be dysregulated between populations within tissue groups (A) liver, (B) skin, and (C) spleen (overlap indicates genes that were dysregulated in more than one population). Genes were classified as dysregulated if they were found to be significantly differentially expressed between uninfected negative control frog samples and Bd-exposed frog samples within-population among tissue samples.

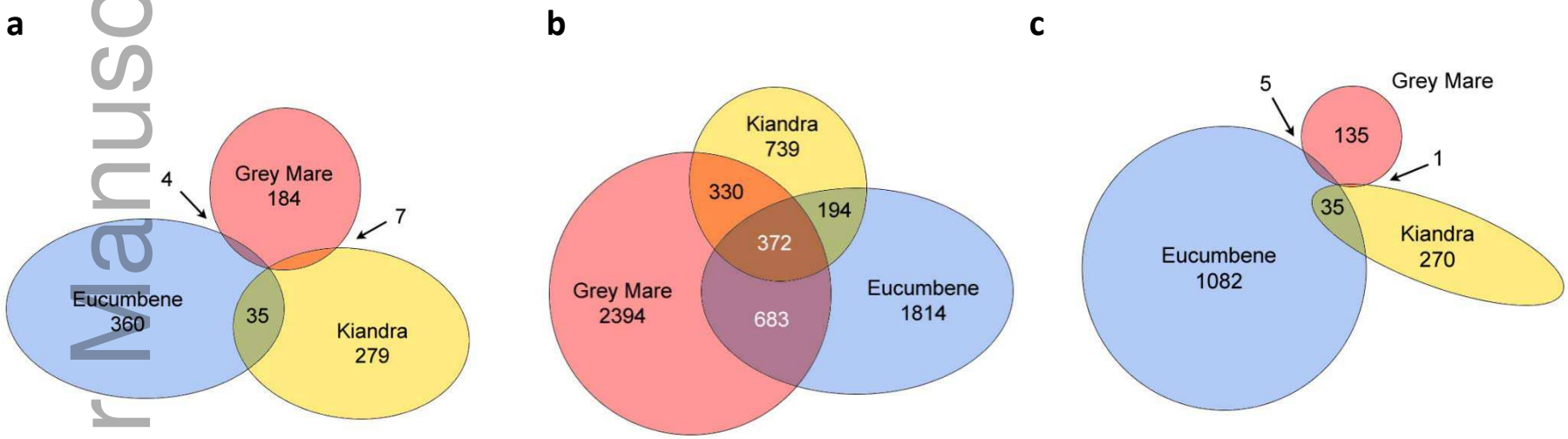

Figure 6. Heatmaps summarizing clusters (labelled at left) of differentially expressed genes (rows) clustered (via Euclidean distance algorithm) by expression pattern between samples within sample groups (days post exposure in columns) in the skin samples from frogs originating from (a) Eucumbene, (b) Grey Mare, and (c) Kiandra. Control samples have been grouped together at the left, and samples within sample groups are

935 arranged from left to right by increasing infection intensity at time of sampling (ZSE). Heatmaps for liver and spleen samples can be found in
936 Supplementary Fig. S5.
937

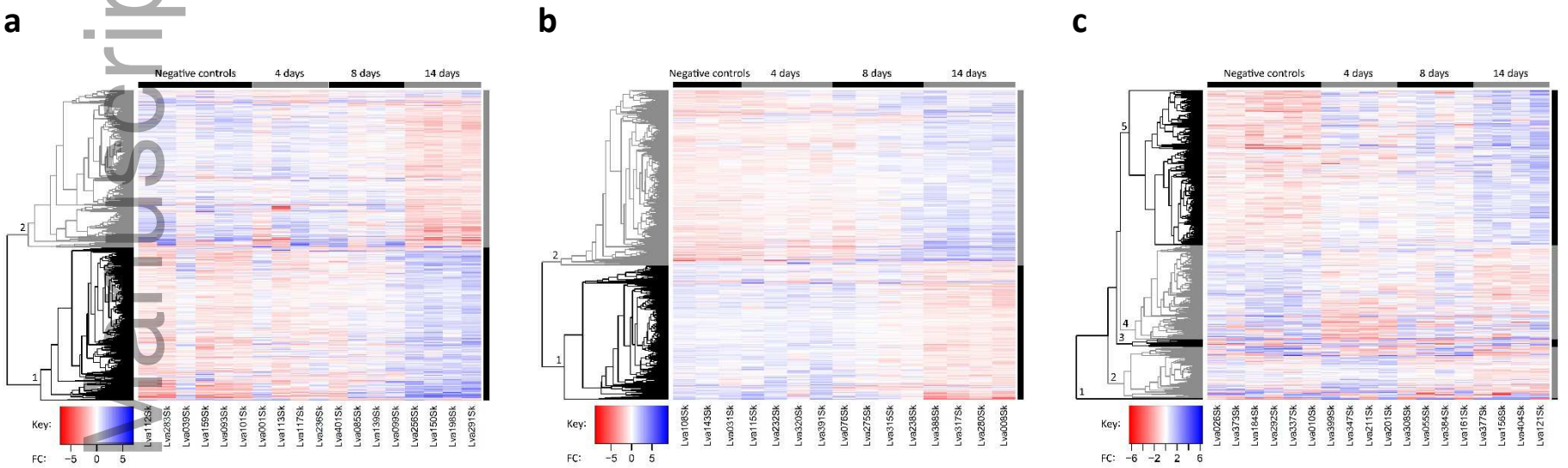

938
939 **Figure 7.** Numbers of up- and down-regulated immune-associated genes comparing uninfected negative control frog samples and Bd-exposed
940 frog samples within-population at sampling periods post exposure, for all populations and tissues. Major immune-associated gene groups have
941 been labeled (using gene search terms; see Supplementary Tables S2-S4 for more details), with numbers of differentially expressed genes in
942 parentheses (where > 10 genes identified). Immune-associated genes were predominantly up-regulated, particularly in skin samples from all
943 three populations at 14 DPE.

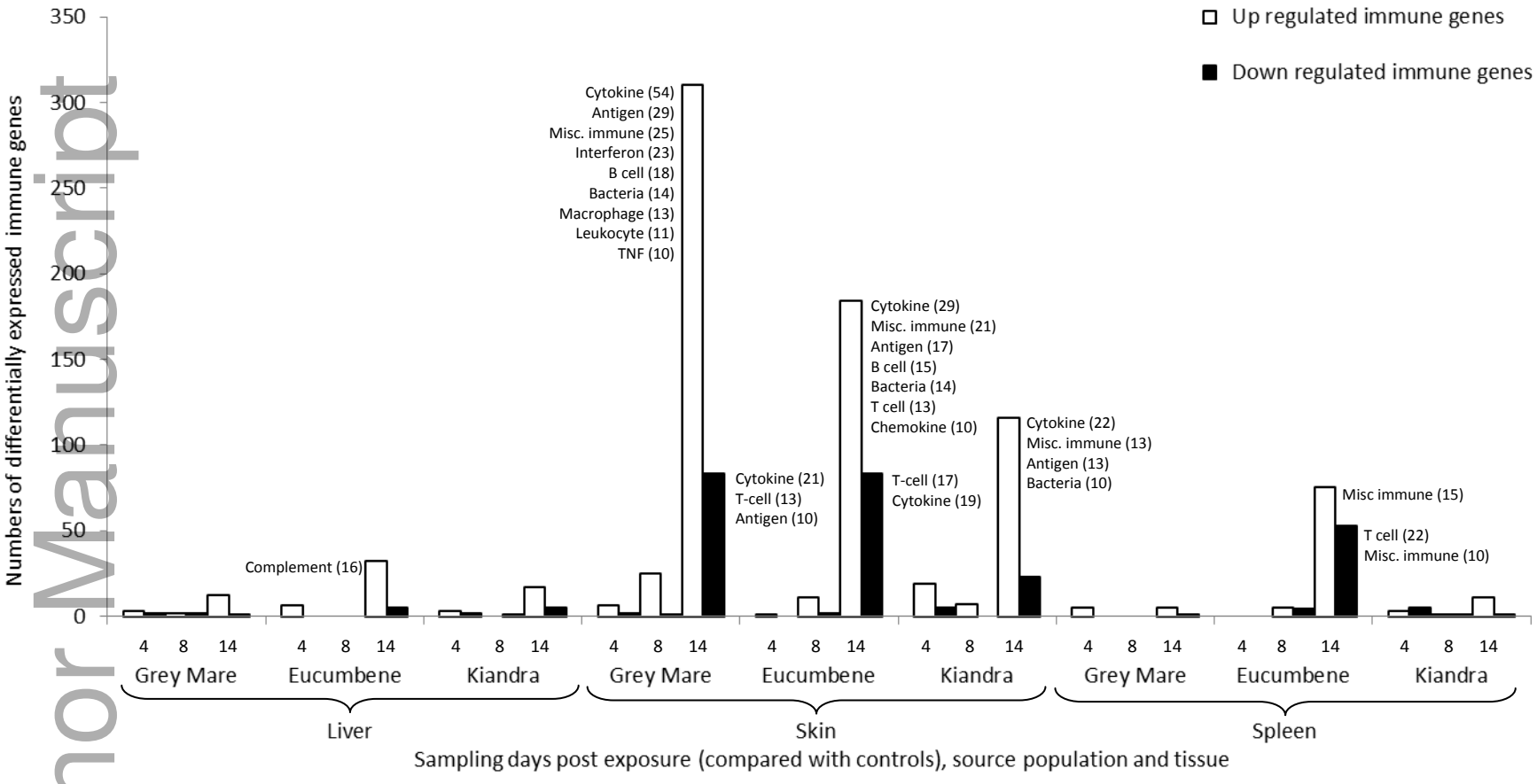

944

Table 1. Demographic characteristics of study subjects (including sample size, treatment group, gender ratios, mean mass pre-euthanasia, mean snout-urostyle length pre-euthanasia and mean and median infection intensity pre-euthanasia).

	Kiandra		Eucumbene		Grey Mare		F value[a]	P value[a]	df[a]
	Exposed	Control	Exposed	Control	Exposed	Control			
Sample size	12	6	12	6	12	3			
Gender[b]	2M, 4F, 6U	2M, 4U	4M, 5F, 3U	5F, 1M	4M, 6F, 2U	1M, 2F			
Mean mass pre-euthanasia	2.99	3.02	3.02	4.05	3.51	3.19	0.938	0.398	2
Mean SUL pre-euthanasia[c]	29.97	30.72	28.80	32.1	32.27	32.03	2.423	0.099	2
Mean ZSE pre-euthanasia[d]	2158.82	0.28	9442.36	0.00	12114.72	0.00	6.592[e]	0.044[e]	2[e]
Median ZSE pre-euthanasia	290.00	0.00	715.00	0.00	910.00	0.00			

[a]Statistics comparing means between populations (pooling exposed and control frog values) using one-way ANOVA, P value and df degrees of freedom; [b]Genders represented by M for males, F for females and U for unknown gender; [c]SUL is snout-urostyle length measured with Vernier callipers; [d]ZSE is zoospore equivalents as measured by qPCR; [e]Statistics refer to $\log_{10}$-transformed uncapped Bd infection intensities ($\log_{10}$[ZSE+1]) between exposed frogs from the three populations at 14 DPE. Other sampling time comparisons were not significant.

Table 2. Summary of mean expression patterns for the genes in each cluster at each time point, and corresponding example significantly enriched GO biological process terms for these clusters, among skin samples (see Supplementary Table S6 for corresponding tables representing results from liver and spleen samples).

Cluster[a] ID	Mean centered log_2(fpkm+1) by sample group[b]				No. of genes	No. GO terms (FDR < 0.05)	Example GO biological process terms[c]
	Control	4 days	8 days	14 days			
SkEuc1	-0.60	-0.19	-0.03	1.12	1285	335	Collagen metabolic process; collagen catabolic process; multicellular organism metabolic process; multicellular organism catabolic process
SkEuc2	0.44	0.15	0.13	-0.95	1325	176	Single-organism intercellular transport; intercellular transport; gap junction-mediated intercellular transport; glycerol transport
SkGre1	0.48	0.53	0.01	-0.90	1430	196	Intracellular transport; single-organism intercellular transport; intercellular transport; gap junction-mediated intercellular transport
SkGre2	-0.73	-0.38	0.05	0.88	1861	277	Collagen metabolic process; collagen catabolic process; multicellular organism metabolic process; multicellular organism catabolic process
SkKia1	-2.43	1.80	0.22	1.63	6	0	N/A
SkKia2	0.21	0.39	-0.20	-0.50	216	86	Cellular potassium ion homeostasis; sodium ion export from cell; establishment or maintenance of transmembrane electrochemical

Cluster[a] ID	Mean centered log_2(fpkm+1) by sample group[b]				No. of genes	No. GO terms (FDR < 0.05)	Example GO biological process terms[c]
	Control	4 days	8 days	14 days			
							gradient; sodium ion export
SkKia3	-0.29	0.45	-0.64	0.63	31	0	N/A
SkKia4	0.52	-0.55	0.13	-0.35	394	9	Peptide cross-linking
SkKia5	-0.68	0.03	0.12	0.87	647	200	Collagen metabolic process; collagen catabolic process; multicellular organism metabolic process; multicellular organism catabolic process

[a]Clusters are defined by Euclidean distance clustering and manually selected using Trinity script `Manually_define_clusters.R` and labelled (see Fig. 6 and Supplementary Fig. S5 for corresponding visual representations); [b]Arithmetic mean of the centered log_2(fpkm+1) expression values grouped by sampling time in days post exposure, from the output of Trinity script `Manually_define_clusters.R` ('Control' group includes all samples from unexposed frogs); [c]Top four most significantly enriched GO Biological Process terms (where applicable) (full list of overrepresented GO terms available in Table S5); [d]N/A indicates that there were no GO Biological Process terms that were significantly enriched with FDR < 0.05 for the respective cluster.

Table 3. Experimental design outlining the number of frogs from each population and treatment group (Bd exposed or unexposed control) sampled at each time point post exposure.

Populations	Exposure – Day 0 Total # exposed (total # control)[a]	Day 4 # exposed sampled (# control sampled)[b]	Day 8 # exposed sampled (# control sampled)[b]	Day 14 # exposed sampled (# control sampled)[b]
Grey Mare (clutch B)	12 (3)	4 (1)	4 (1)	4 (1)
Eucumbene (clutch D)	12 (6)	4 (2)	4 (2)	4 (2)
Kiandra (clutch B)	12 (6)	4 (2)	4 (2)	4 (2)
Total	36 (15)	12 (5)	12 (5)	12 (5)

[a]Total number of unexposed control frogs shown in parentheses; [b]Number of unexposed control frogs sampled shown in parentheses.

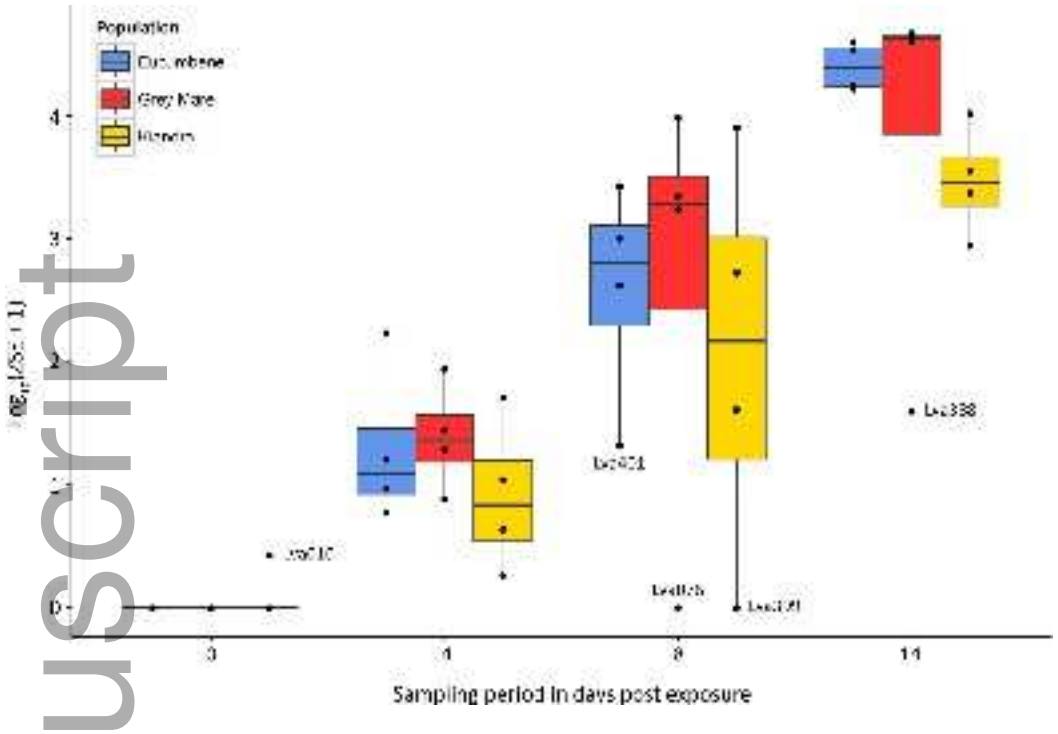

mec_14493_f1.tif

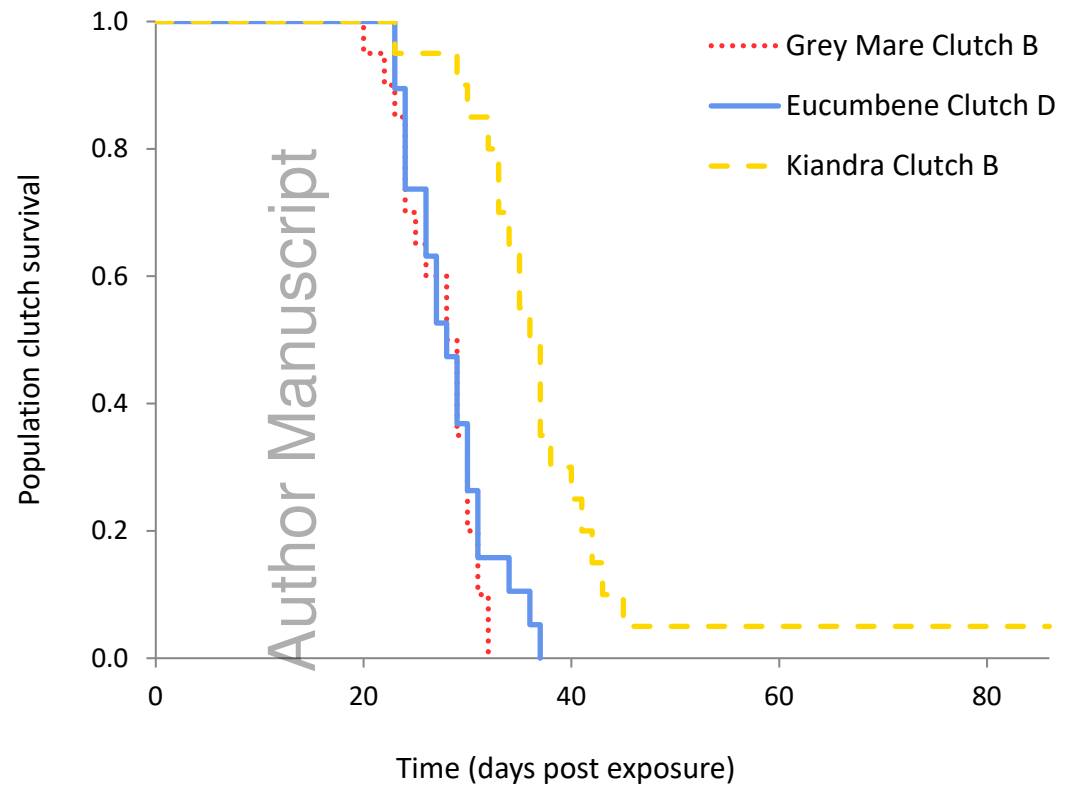
Grey Mare Clutch B
Eucumbene Clutch D
Kiandra Clutch B
Population clutch survival
1.0
0.8
0.6
0.4
0.2
0.0
0
20
40
60
80
Time (days post exposure)
Author Manuscript